FINITE ELEMENT ANALYSIS OF GUSSET PLATE CONNECTION DESIGN FOR COLD-FORMED STEEL FRAMES

Aloysius Yoke Khing Ng[1], Yeong Huei Lee[1], Tina Chui Huon Ting[1], Cher Siang Tan[2], Shahrin Mohammad[2]

[1]Department of Civil and Construction Engineering, Faculty of Engineering and Science, Curtin University Malaysia, CDT 250, 98009 Miri, Sarawak, Malaysia.
[2]School of Civil Engineering, Faculty of Engineering, Universiti Teknologi Malaysia, 81310 Johor Bahru, Malaysia.

Abstract — The application of cold-formed steel sections has been extended from secondary members to primary structural members in recent years. This increases the use of gusset plate connections in cold-formed steel since it is a common connection used in steel structures. However, current design codes on connection design do not have a comprehensive method to consider the effects due to the buckling of the thin cold-formed steel sections. Therefore, it is important to develop a more accurate model to predict the capacity of cold-formed steel connections. This paper aims to propose an equation for gusset plate beam-to-column connection using finite element models. Finite element models have been developed and compared with existing test results. The failure mode and ultimate strength of the numerical models are similar to the experimental results. The validated finite element models are then used to study the effects of gusset plate thickness, effects of cold-formed steel section depth and thickness, and the effects of bolt size and spacings. Elastic and plastic stiffnesses are obtained from the developed models. The connection behavior followed a typical elastic-plastic curve according to the connection ductility and failure mode. An empirical model is developed from the finite element models to predict the joint behavior of gusset plate beam-to-column connection for cold-formed steel structures. AS 4600 may have underestimated the initial stiffness of the connection.

1.0 INTRODUCTION

Gusset plate connections, commonly found in steel structures, are used for transferring loads between structural members [1]. Due to the lack of comprehensive design method for cold-formed connection, design method for hot-rolled connection is used without considering the effects of buckling of cold-formed steel [2-4]. Overestimated structural performance [5] and out-of-plane deflection [6] are common in cold-formed steel structures.

Moment rotation curve is the most suitable behaviour for representing the joint analysis [7]. Cold-formed connections were found to be unable to achieve their full moment capacity before failing due to buckling. An opportunity is present for further research into the design of a cold-formed connection. Cold-formed gusset plate is a common and simple connection which can be adopted into most light steel frame designs and is thus a good starting point. Previous research conducted on cold-formed gusset plate connections [8-10] revealed its behaviour as a semi-rigid connection and its inability to achieve its flexural capacity before failing in buckling. The usage of a gusset plate section with a lower thickness than the connected member could lead to the premature failure alongside a lowered moment capacity.

There are many methods which can be used to predict moment rotation behaviour, including component method in Eurocode, empirical formula, finite element analysis, analytical model and experimental investigation. The traditional method of analysis is through formulae recommended by standard codes of practice. However, for cold-formed steel connections, these formulae are not reliable as there are no recommendations to adopt hot-rolled connection formulae for cold-formed connections. This issue is also investigated by Rogers and Hancock (1999) [11] where they found that the formulae by AS4600, AISI and Eurocode are not suitable to predict the bearing

capacity of cold-formed steel connection. Huynh, Pham, and Hancock (2020) [12] recommended a reduction in the capacity factor from AS4600 when used for cold-formed steel screwed connections in bearing.

Therefore, this research is conducted to develop a prediction model for gusset plate connection used in cold-formed steel structures. There are three stages of progression: model validation, parametric study and equation development. In the parametric study, geometrical effects of gusset plate, cold-formed steel section and bolt on the joint moment-rotation performance is investigated. An empirical formula is then developed to predict the joint capacity.

2.0 FINITE ELEMENT MODEL DEVELOPMENT

2.1. Model description

All elements in this model are modelled as C3D8R deformable solid elements. The results from previous experimental results [8] were used to validate the finite element models. The cold-formed steel tensile strength is obtained from the same reference and the bolt capacity is set to 640 MPa ultimate strength for grade 8.8 [8]. The boundary conditions and material properties were similar to the experimental models. For contact interactions, a value of 0.19 is used for the tangential behaviour and hard contact is assigned for the normal behaviour with separation allowed for after contact. Finite sliding is assigned for the contacts between each surface of the parts. Based on the mesh size recommendations from previous studies [3-4], the model were meshed and partitioned for hex-dominated mesh with 40 mm size.

2.2. Detail of the specimen

The top of the column was pinned and the bottom of the column was set as a roller support. The loading was applied upwards at 1160mm from the edge of the beam as shown in Figure 1. The gusset plate is 12 mm in thickness with yield and ultimate strengths of 442 MPa and 570 MPa [8]. The bolt spacings are 200 and 150 mm for beam channel sections with gusset plate and column with gusset plate respectively [8]. The bolts are 12 and 16 mm diameter, as indicated in the specimen name. C15015 indicated 150 mm section depth and 1.5 mm section thickness.
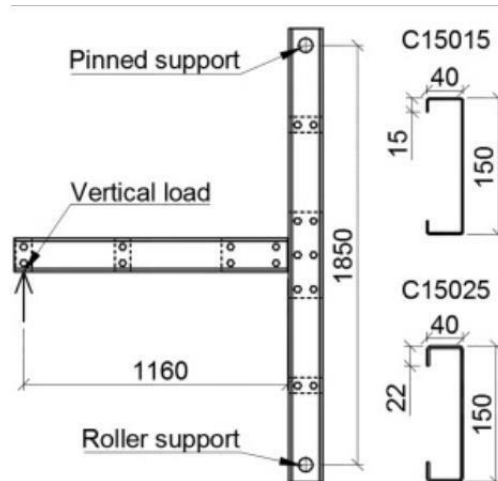

**Figure 1** Experimental specimen and setup [8]

2.3. Model validation

The moment-rotation curve obtained from finite element software, ABAQUS was used to compare the experimental results from [8]. Figure 2 showed the moment-rotation performance comparison of specimens for C15015 M12, C15025 M12 and C15015 M16. The model validation showed that the models were able to accurately replicate the results of the experiment. The greatest differenceis 13.5% higher than the experimental results for specimen C15015 M16 where the FE model resulted in 1.106kNm.. All the models failed at about the same maximum loading with the same failure modes at failure compared to the experiments. Both C15015 M12 and
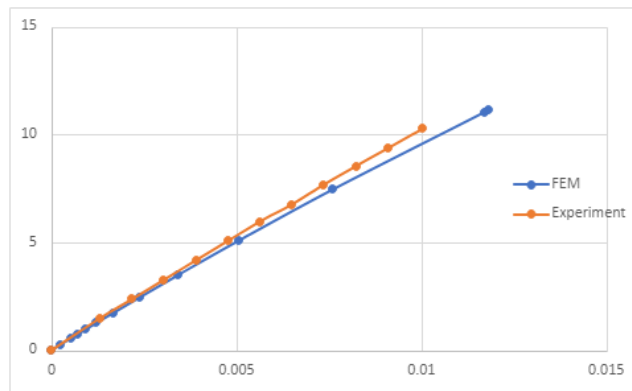
C15015 M16 models failed due to local buckling of the beams. The C15025 M12 T12 models failed due to bearing deformations around the holes and local buckling of the beam.
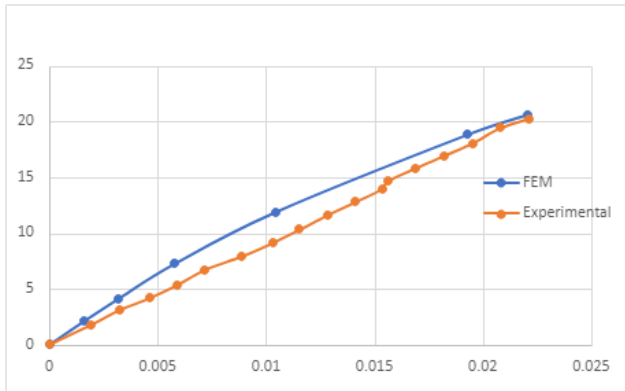

(a)
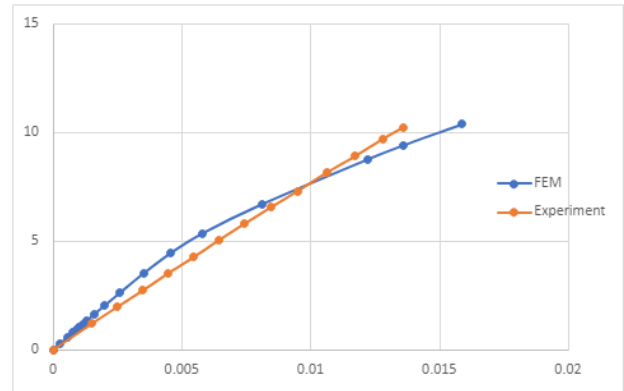
(b)

(c)

Figure 2 Moment rotation curve of (a) C15025 M12, (b) C15015 M12 and (c) C15015 M16

2.3.1. Failure mode

The failure mode of a cold-formed steel structure may occur at beams, columns, bolts, and gusset plate. The identified failure mode was compared to the highest stress area in the simulation. Table 1 shows the failure mode from experimental and simulation results. Figure 3 shows high stress in the finite element model at location were bolt shear failure occurred during the experiment.Bearing deformations around the holes and local buckling of the beam were also observed in the model. The stress contour around the thread of the bolts were with the highest stress. This failure mode occurs when the shear capacity of the bolt is less than the critical capacity of the section which makes the structure fail with bolt in shear.
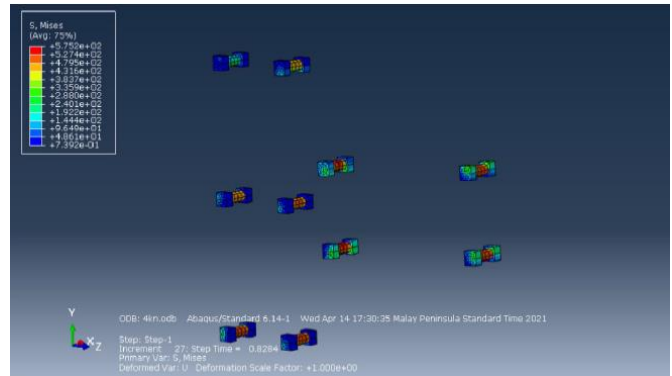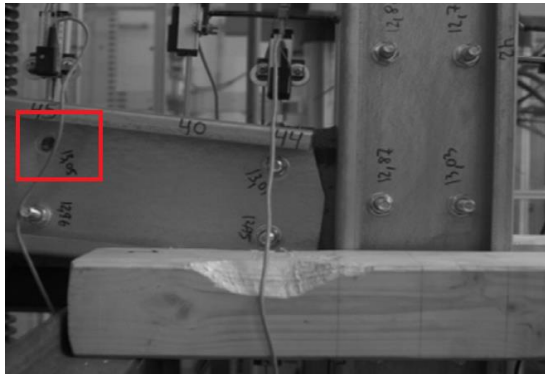
(a)   (b)

Figure 3 Bolt shear failure of C15025 M12 for (a) experimental study and (b) finite element model

2.3.2. Ultimate capacity

Table 1 shows the comparison of results between experimental study from [8], theoretical analysis from AS4600 design specification and finite element analysis. The finite element results achieve good agreement with the experimental results. The greatest difference in maximum moment capacity found between the finite element model and the experimental model was 0.776 kNm. The maximum rotation of the finite element model was also found to be close to the maximum rotation of the experimental models with a maximum difference of 0.00484 radian. However, the difference was higher when compared to the prediction from AS4600 with AS4600 yield higher results for both maximum moment capacity and maximum rotation.

Table 1 Comparison of maximum moment and rotation

Specimens	EXP		FEM				AS4600			
	Max. Moment, kNm	Max. Rotation, 10^{-3} rad	Max. moment		Max. rotation		Max. moment		Max. rotation	
			kNm	% *	10^{-3} rad	%*	kNm	%*	10^{-3} rad	% *
C15015M12	10.224	13.58	11.0	7.59	18.42	35.64	11.957	16.95	27.97	105.96
C15025M12	20.220	22.08	20.0	1.09	22.07	0.05	12.604	37.67	29.48	33.51
C15015M16	10.270	10.06	10.8	5.16	11.82	17.50	11.957	16.43	27.97	178.03

*% difference with EXP

3.0 PARAMETRIC STUDY

The parameters of gusset plate thickness, section depth, section thickness, bolt size and bolt spacings were investigated. The same material properties and boundary conditions were applied in this parametric study.

3.1. Effect of gusset plate thickness

The gusset plate thickness was increased with 2 mm increments from 2 to 16 mm. The performance was shown in Figure 4. The maximum moment was found to increase with the gusset plate thickness, as indicated in Figure 5. The maximum moment increased from 9.72 kNm at 2 mm thickness to 16.89 kNm at 16 mm thickness. The maximum rotation decreased from 0.03864 radians to 0.1989 radians from 8 to 10 mm thickness where there was only a small change in the overall rotation even though the gusset plate thickness increased. The failure mode of the models was found to be due to local buckling of the C-section beams after 6 mm thickness of gusset plate. An increase in the thickness of the gusset plate resulted in the decrease in ductility of the joint [13].
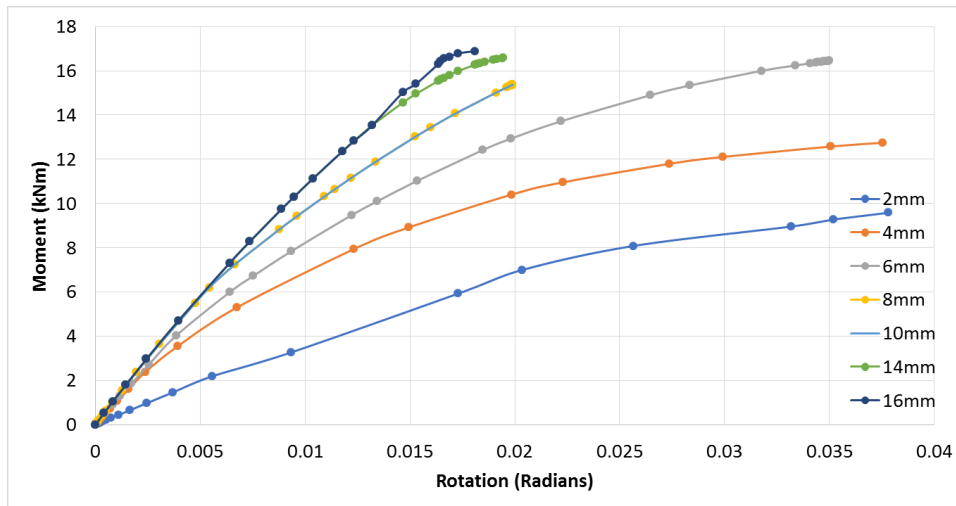
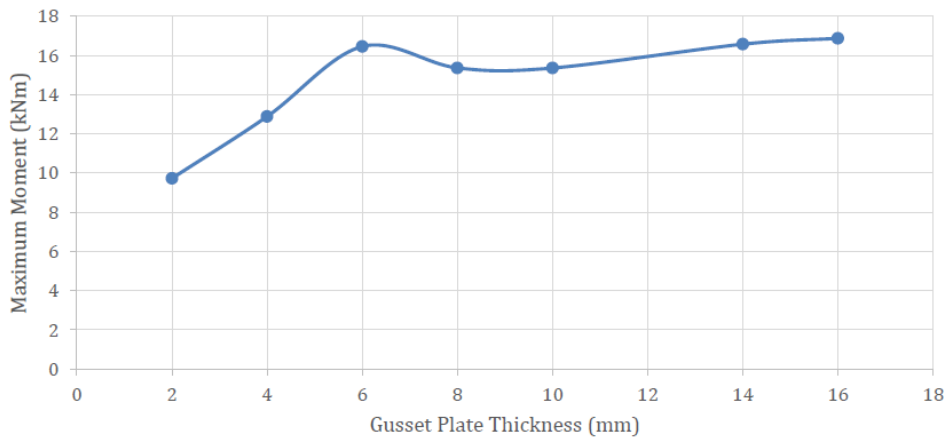**Figure 4** Moment-rotation performance of gusset plate connection for gusset plate thickness of 2 to 16 mm

Figure 5 Maximum moment of various gusset plates

3.2. Effect of sectional thickness and depth

The flange of the section remained the same as C15015 and the depth and the thickness were varied for parametric investigation. The maximum moment increased as the C-section thickness increased up to 8 mm thickness, as in Figure 6. When the maximum moment remained constant at around 37 kNm, the failure mode changed from local buckling of the beam to bolt shear failure with bearing deformations around the bolt holes. This is also observed on the finite element models.

The finite element models prediction exceeded the 20.2 kNm failure moment from the experiment which failed due to bolt shear because the moment-rotation curve of the experiment is still in the elastic behaviour at failure. It is suspected that the failure moment was able to reach higher values as the test specimens have yet to develop plastic behaviour as shown on the moment-rotation curve.

The maximum rotation increased as the C-Section thickness increased up to 3mm thickness when the rotation fluctuated around 0.06 Radians. The failure mode changed from local buckling of C-Section to bolt shear failure with bearing deformation around the holes and beam buckling. The increased C section thickness provided additional restraint against local buckling, which made the bolt shear the critical capacity.
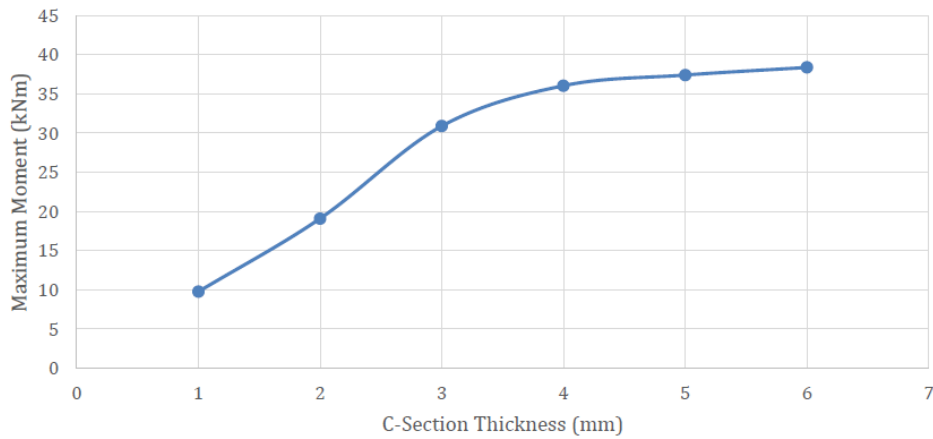
Figure 6 Maximum moment of various sectional thickness

The increase in the depth of the C-section decrease the maximum moment as the maximum moment was governed by the failure mode due to local buckling, as shown in Figure 7. The maximum moment decreased from 17.51 kNm at 200 mm section depth to 14.00 kNm at 300 mm section depth. The maximum moment decreased as the section depth increased, because section with larger depth is more vulnerable to local buckling. The maximum rotation decrease as the section depth increase. The maximum rotation decreased from 0.01813 radians to 0.0093 radians. The increase in section depth resulted in additional web depth which was able to resist forces and reduce the overall deflection of the members.
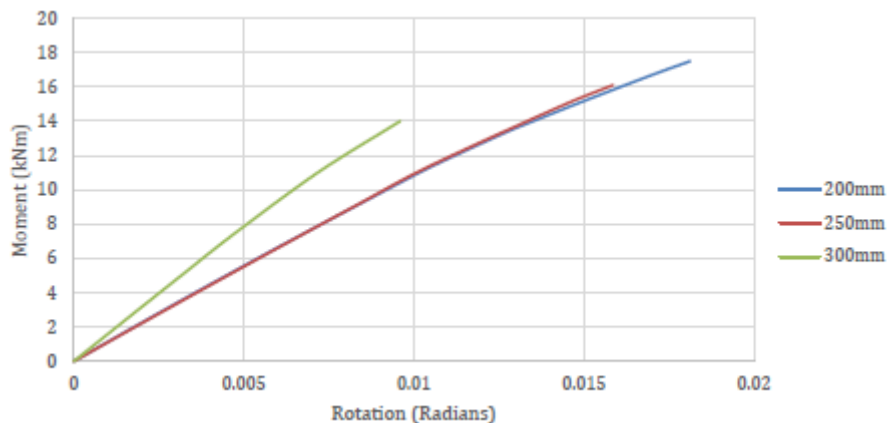

Figure 7 Moment-rotation behaviour with various sectional depth

3.3. Effect of bolt size and spacing

The C15015 was used in this study with different bolt sizes and spacings. The bolt sizes which were involved in the parametric study are M16, M20 and M24. The increase of bolt size had very little impact on the stiffness of the structure, as shown in Figure 8. Increasing bolt size to M24 only increased the maximum moment by 0.25 kNm. The rotation was reduced by up to 0.01 radians as the bolt size increased. The maximum rotation (33%) was affected more than the maximum moment (4.6%) as the structure became less ductile with increased bolt size.
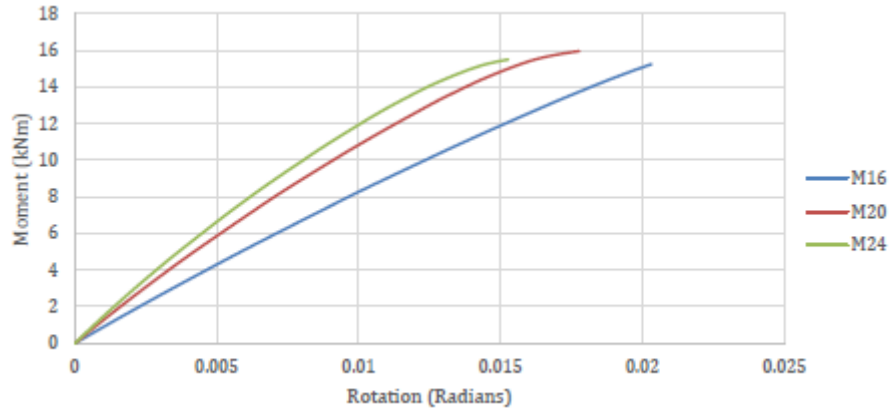
Figure 8 Moment-rotation behaviour of bolt sizes of 16, 20, 24 mm

The studied range of bolt spacings is between 50 to 200 mm with 50 mm increment. The maximum moment increased as the bolt spacing increased, up to 100 mm bolt spacing where there was minimal increment to the maximum moment, as shown in Figure 9. The maximum rotation increased as the bolt spacing increased. The maximum moment increased from 14.94 kNm with 50 mm bolt spacing to 19.82 kNm with 200 mm bolt spacing. The maximum rotation decreased from 0.01617 radians to 0.02305 radians at an additional 200mm spacing. The gusset plate size was increased to ensure consistency in the parametric study. The increase in dimensions of the gusset plate decreased the ductility of the joint and increased the maximum moment capacity of the models.
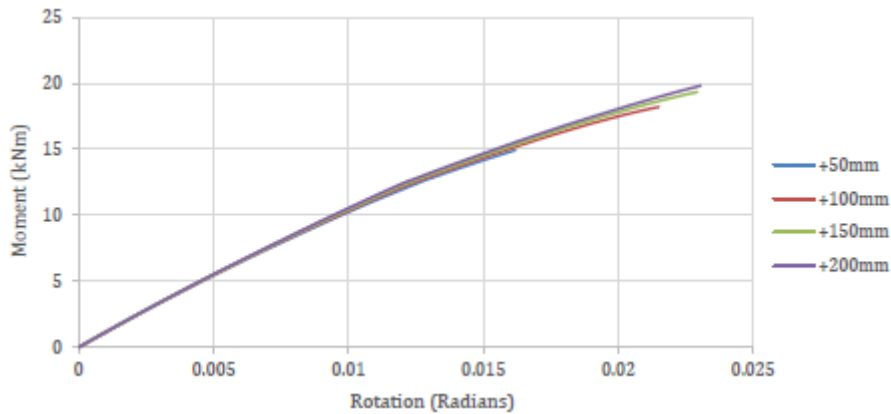

Figure 9 Moment-rotation performance of various bolt spacings

4.0 PREDICTION MODEL DEVELOPMENT

4.1. Initial stiffness

The initial or elastic stiffness was extracted from the moment rotation curves from the model development as well as the parametric study, typically in the range of 0 to 0.005 rad rotation. The least square method was then used to obtain the elastic stiffness of the joint as in Eq. 1.

$$k_e = 1.3 \times 10^{-3} \, G \tag{1}$$

k_e is the initial stiffness and G is the geometrical property (given by Eq. 2)

$$G = t_{cf}^{1.15} \times t_{gp}^{1.17} \times D_b^{1.62} \tag{2}$$

t_{cf} is the thickness of column flange, t_{gp} is the thickness of gusset plate and D_b is the beam's depth

65

4.2. Secant stiffness

The secant or plastic stiffness is the stiffness in the plastic region and is normally less than elastic stiffness. They were extracted from the moment rotation curves from the model development (section 2) as well as the parametric study (section 3), ranged from 0.005 rad to maximum rotation. The least square method was then used to obtain the elastic stiffness of the joint. The secant stiffness obtained was proposed as Eq. 3.

$$k_p = 1.0 \times 10^{-3} \, G \tag{3}$$

4.3. Joint moment capacity prediction

The curve fitting constant in the equation by [14] was determined through trial and error. The Moment Rotation curve from the simulation was able to fit the curve when the curve fitting constant was equal to 0.1. As the magnitude of the curve fitting constant, C increased, the moment rotation curve started to deviate further away from the experimental results. The initial and secant stiffnesses took values from the least square method introducing additional factors, with 0.41 being introduced into ke and 0.35 being introduced to kp. Using a curve fitting constant of 0.1 the proposed equation for joint moment capacity prediction, is as in Eq.4.

$$M_j = \left[1 - e^{-\frac{(-0.41k_e + 0.35k_p + 0.1\varphi)}{M_{j,p}}} \right] + 0.35k_e\varphi \tag{4}$$

M_j is the moment of joint, $M_{j,p}$ is the maximum moment of joint, k_e is the initial stiffness, k_p is the secant stiffness, φ is the joint rotation. This empirical equation is valid for the section thickness up to 6 mm, gusset plate thickness up to 16 mm, section depth up to 300 mm and bolt diameter up to 24 mm.

4.4. Prediction model validation

The moment capacity calculated for the C15025 M12 experimental model using AS 4600 yielded a maximum moment of 12.60kNm and maximum rotation of 0.02948 radians. The experimental results provided a maximum moment of 20.22kNm and 0.02276 radians. The maximum moment predicted through AS 4600 was significantly lower than the experimental results and considered conservative which still exhibit elastic behaviour during failure.

Using the proposed equation in Eq. 4, a maximum moment of 27.66kNm and maximum rotation of 0.02997 radians was obtained. The maximum rotation predicted using the proposed formula included the elastic and plastic stiffness of the material which provided a greater moment capacity.

Figure 10 reveals that the maximum rotation predicted by both the AS 4600 calculations and the proposed equation were similar. However, the stiffness gradient of the AS 4600 calculations deviated far away from the experimental results. The proposed equation was able to produce a similar stiffness gradient. However, the proposed equation computed a maximum moment of 15.06kNm greater than AS4600 prediction. This is because the proposed equation takes into account the secant stiffness of the connection and the experimental model failed while exhibiting signs of elastic behaviour on the moment rotation curve.
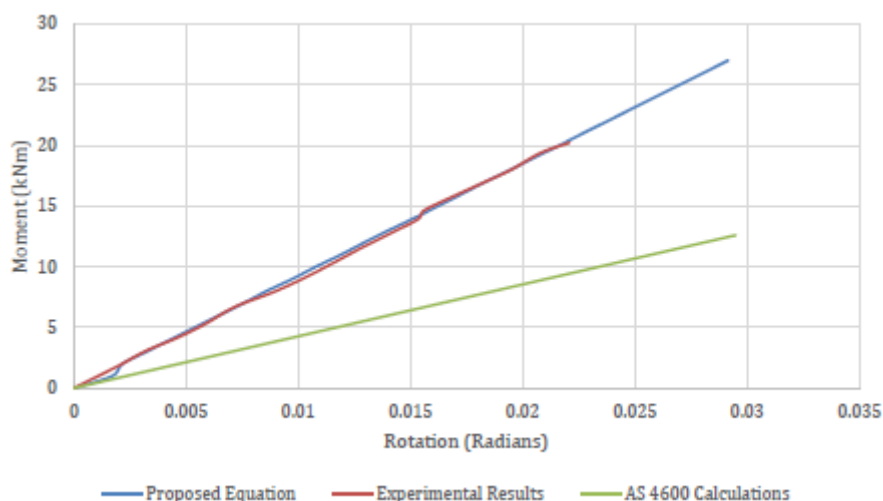
Figure 10 Comparison of proposed prediction model, experimental data and AS4600 design specification for C15025 M12

5.0 CONCLUSIONS

Finite element models were developed and validated with the experimental results from Bučmys et al. (2018). The finite element models were developed using fully plastic properties and using the same setup and boundary conditions as in the experimental setup. The finite element model exhibits similar failure modes compared to the experiment with a maximum difference of 1.106kNm found over all 3 models.

Parametric study has been conducted for geometrical properties, gusset plate thickness, C-section depth, C-section thickness, bolt size and bolt spacing. The parametric study revealed that increasing the thickness of the beam has the most significant increase to the maximum moment capacity as the beam changes the failure mode from local buckling to bolt failure. All the models in the parametric study concluded that the cold-formed gusset plate was not the critical component in the structure.

The equation for the design of maximum moment of cold-formed gusset plate connection has been proposed. The factors for initial stiffness and secant stiffness were obtained by using the least square method. The proposed equation was determined through fitting the results from the finite element models to match the experimental results by introducing a curve fitting factor of 0.1. The application of the proposed equation in 3 separate experimental models produced results of higher maximum moment due to the secant stiffness.

Conflicts of Interest

The authors declare that there are no conflicts of interest regarding the publication of this paper.

Acknowledgement

The authors would like to acknowledge the support provided by Curtin University Malaysia.

References

[1]   Vivek, K. S., Priyanka, U. K. L., Reddy, C. R. K., & Ram, K. S. S. (2019). Non–linear finite element analysis of mild steel gusset plates. Materials Today: Proceedings, 18, 3726-3732. https://doi.org/10.1016/j.matpr.2019.07.307
[2]   Lee, Y. H., Tan, C. S., Tahir, M., & Mohammad, S. (2012). Numerical modelling and validation of light gauge steel top-seat flange-cleat connection. Journal of Vibroengineering, 14(3), 1104-1112.
[3]   Tan, C. S., Lee, Y. H., Lee, Y. L., Mohammad, S., Sulaiman, A., Tahir, M. M., & Shek, P. N. (2013). Numerical simulation of cold-formed steel top-seat flange cleat connection. Jurnal Teknologi, 61(3), 63–71. https://doi.org/10.11113/jt.v61.1769
[4]   Lee, Y. H., Tan, C. S., Mohammad, S., Lim, J. B. P., & Johnston, R. (2015). Numerical study of joint behaviour for top-seat flange cleat connection in cold-formed steel structures. Scientia Iranica, 22(4), 1554-1566.
[5]   Ghandi, E. & Shirin E. N. (2020). Flexural-torsional buckling of cold-formed steel columns with arbitrary cross-section under eccentric axial load. Structures, 28, 2122-2134. https://doi.org/10.1016/j.istruc.2020.09.081

[6]   Lee, J., Byun, N., Lee, Y., Kang, S. Y., & Kang, Y. -J. (2021). Experimental and numerical evaluations of local buckling in thin-walled UHPFRC flanges. Thin-Walled Structures, 163, 107662. https://doi.org/10.1016/j.tws.2021.107662

[7]   Shi, G. & Chen, X. (2017). Moment-rotation curves of ultra-large capacity end-plate joints based on component method. Journal of Constructional Steel Research, 128, 451-461. https://doi.org/10.1016/j.jcsr.2016.09.012

[8]   Bučmys, Ž., Daniūnas, A., Jaspart, J. -P., & Demonceau, J. -F. (2018). A component method for cold-formed steel beam-to-column bolted gusset plate joints. Thin-Walled Structures, 123, 520-527. http://dx.doi.org/10.1016/j.tws.2016.10.022

[9]   Aminuddin, K., Saggaff, A., Tahir, M. M., Shek, P. N., Sulaiman, A, Firdaus, M., & Aghlara, R. (2019). Analytical and experimental investigation on slip-in gusset plate connection for double c-channel sections of cold-formed steel. The Open Civil Engineering Journal, 13, 210-217. https://doi.org/10.2174/1874149501913010210

[10]   Firdaus, M., Saggaff, A., Tahir M. M., Aminuddin, K. M., Ngian, S. P., Siang, T. C., Ali Salih, M. N., Mohammadhosseini, H., & Sulaiman, A. (2021). Behavior of partial strength of beam-to-column connection with gusset plate for cold-formed steel sections. ASEAN Engineering Journal, 10(2), 99-114. https://doi.org/10.11113/aej.v10.16601

[11]   Rogers, C. A. & Hancock, G. J. (1999). Bolted connection design for sheet steels less than 1.0 mm thick. Journal of Constructional Steel Research, 51(2), 123-146. https://doi.org/10.1016/S0143-974X(99)00018-8

[12]   Huynh, M. T., Pham, C. H., & Hancock, G. J. (2020). Experimental behaviour and modelling of screwed connections of high strength sheet steels in shear. Thin-Walled Structures, 146, 106357. https://doi.org/10.1016/j.tws.2019.106357

[13]   Liu, Y., Shan-Shan, H., & Ian, B. (2021). Fire performance of axially ductile connections in composite construction. Fire Safety Journal, 121, 103311. https://doi.org/10.1016/j.firesaf.2021.103311

[14]   Yee, Y. L. & Robert, E. M. (1986). Moment-rotation curves for bolted connections. Journal of Structural Engineering, 112(3), 615-635. https://doi.org/10.1061/(ASCE)0733-9445(1986)112:3(615)